Energy Materials

Supplementary Materials

Bismuth chloride additive regulated anode interphase and kinetics in manganese-ion batteries

Yuxuan Zhang[#], Ying Zhang[#], Shize Liu, Hexige Wuliji, Huirong Liu, Aruuhan Bayaguud*

School of Materials Science and Engineering, Inner Mongolia University of Technology, Hohhot 010051, Inner Mongolia, China.
[#]Authors contributed equally.

***Correspondence to:** Prof. Aruuhan Bayaguud, School of Materials Science and Engineering, Inner Mongolia University of Technology, No. 49 Aimin Street, Xincheng District, Hohhot 010051, Inner Mongolia, China. E-mail: jinaruhan@imut.edu.cn

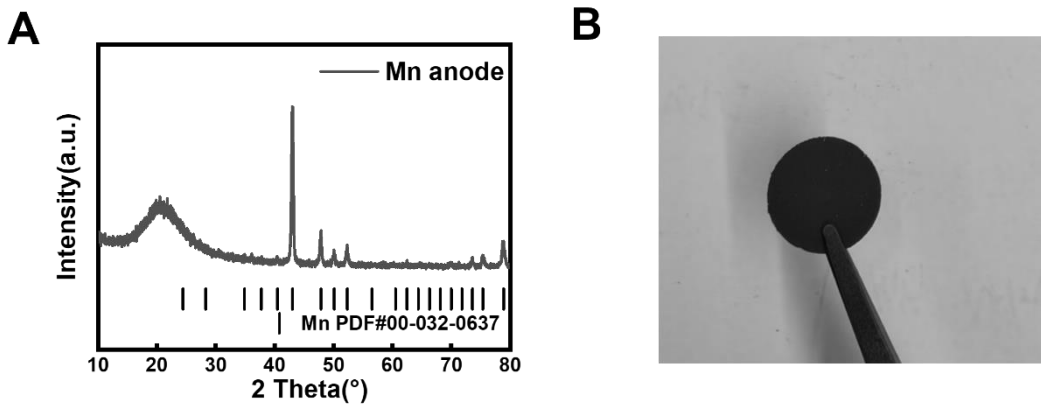

Supplementary Figure 1 A: XRD pattern; B: Optical photograph of the Mn anode. (Photograph taken by the authors.)

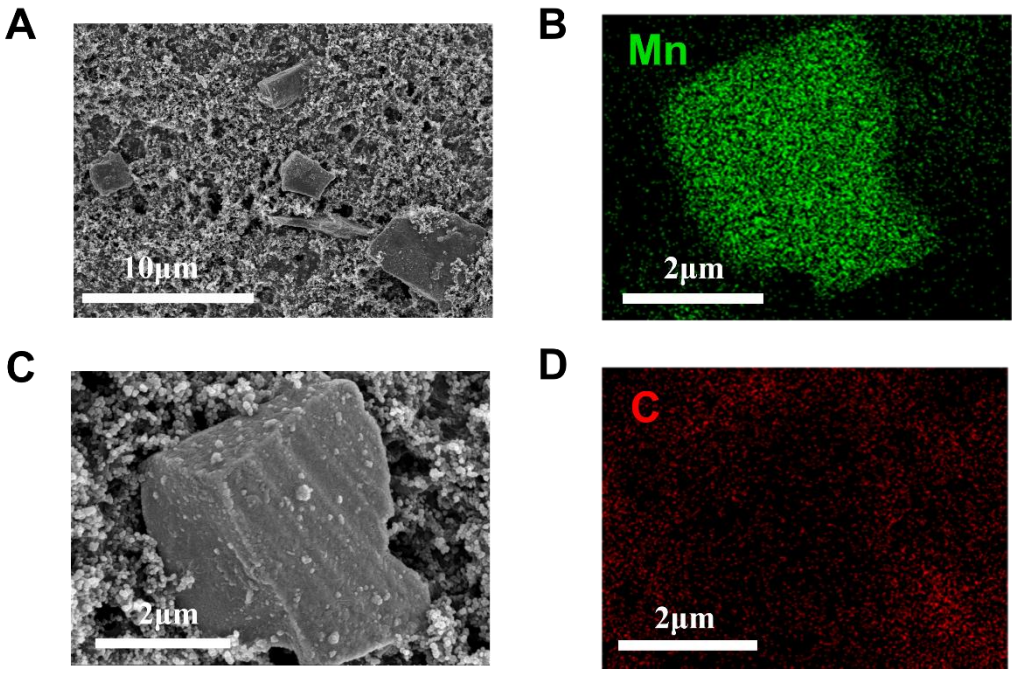

Supplementary Figure 2 A and C: SEM images of the Mn anode; B and D: Corresponding EDS elemental mappings of the Mn anode.

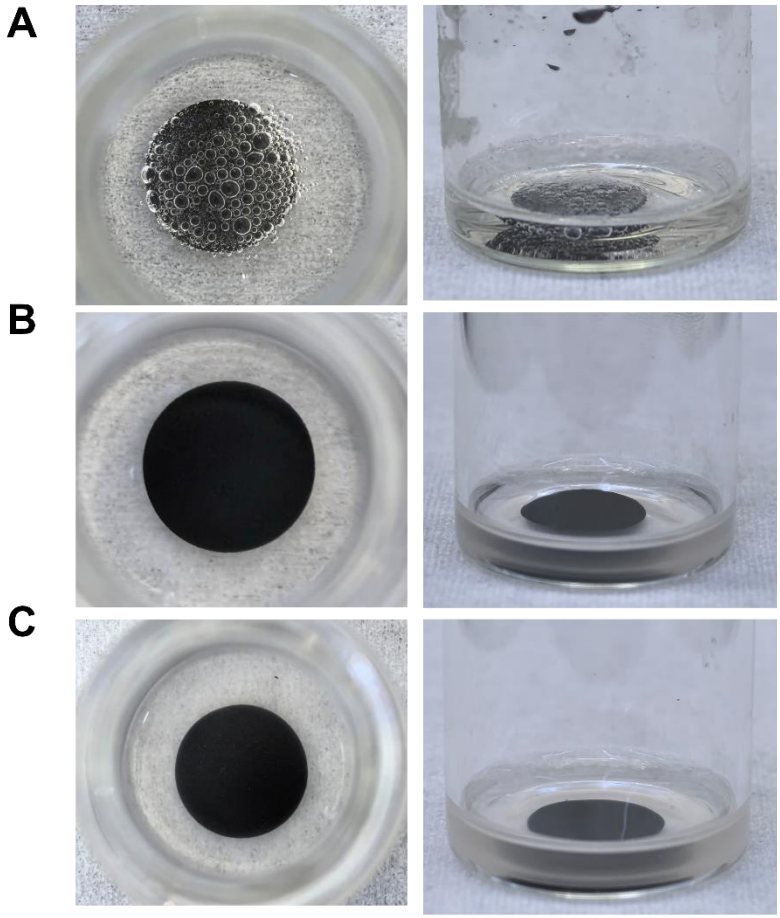

Supplementary Figure 3 Optical photographs of Mn after immersion in different electrolytes: A: aqueous electrolyte (AE), B: G2-$Mn(OTf)_2$, and C: G2-$BiCl_3$. (Photograph taken by the authors.)

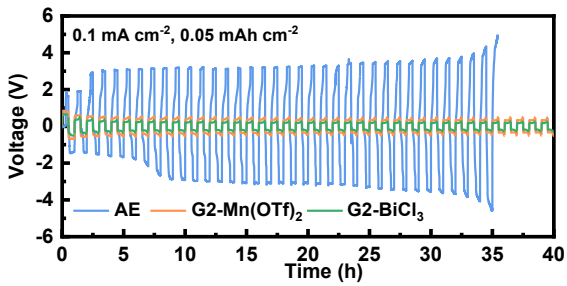

Supplementary Figure 4 Comparison of long-term cycling stability of Mn||Mn symmetric cells with different electrolytes.

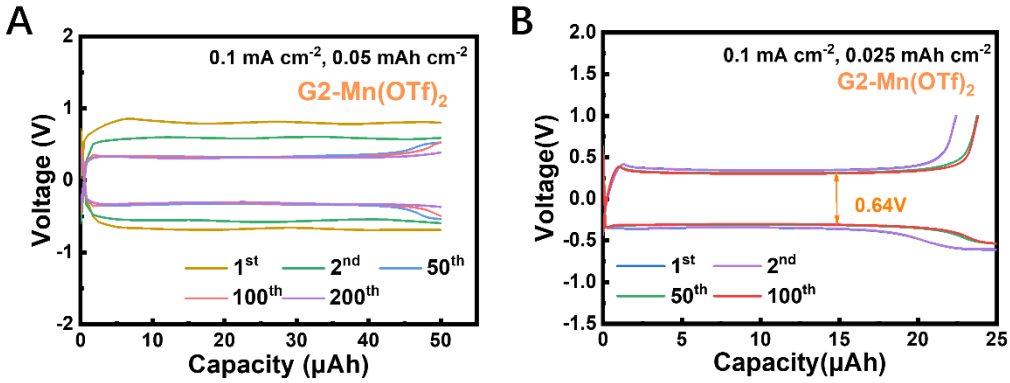

Supplementary Figure 5 A: Voltage profiles at selected cycles for the Mn||Mn symmetric cell with G2-Mn(OTf)$_2$ electrolyte; B: Voltage profiles at selected cycles for the Mn||Cu asymmetric cell with G2-Mn(OTf)$_2$ electrolyte.

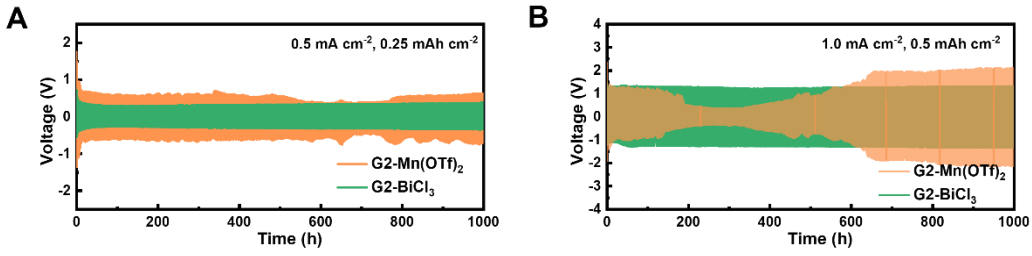

Supplementary Figure 6 Long-term cycling performance of Mn||Mn symmetric cells with different current densities and areal capacities.

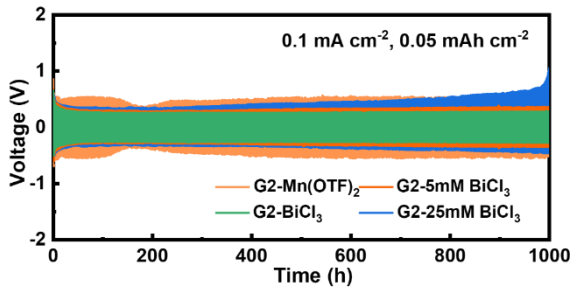

Supplementary Figure 7 Long-term cycling performance of Mn||Mn symmetric cells with different electrolytes.

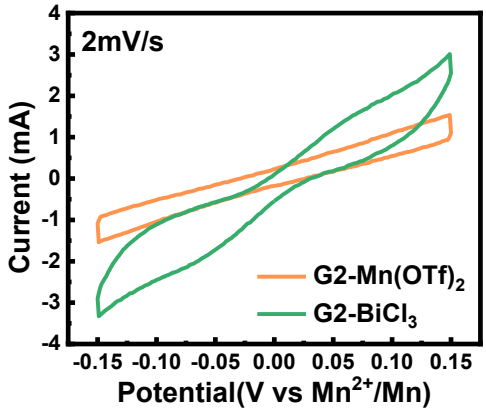

Supplementary Figure 8 CV curves of Mn||Mn symmetric cells with different electrolytes.

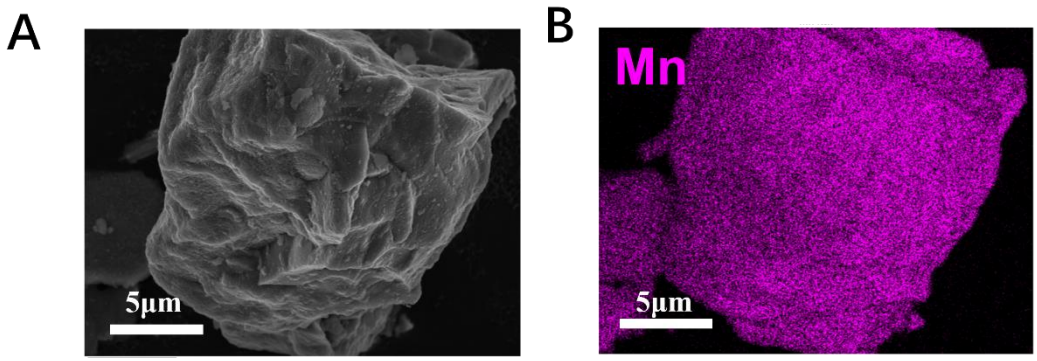

Supplementary Figure 9 A: SEM image and B: corresponding EDS elemental mapping of Mn powder after immersion in the G2-Mn(OTf)$_2$ electrolyte.

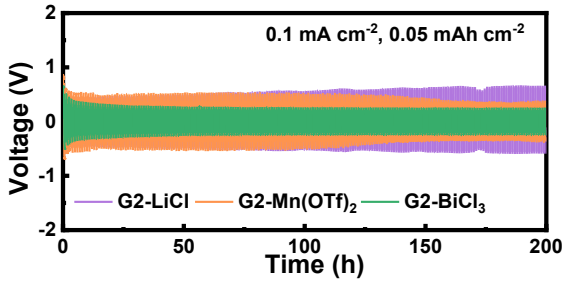

Supplementary Figure 10 Extended cycling performance of Mn||Mn symmetric cells with different electrolytes.

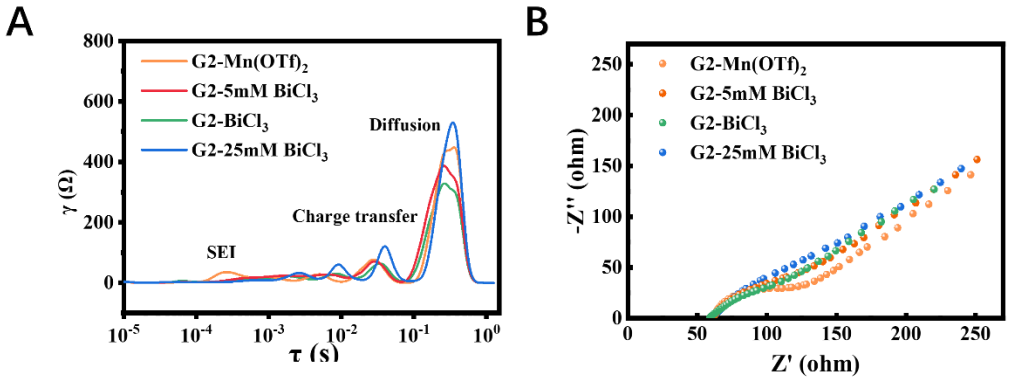

Supplementary Figure 11 EIS and DRT analyses of Mn||Mn symmetric cells with different electrolytes. A**:** Raw EIS spectra without equivalent-circuit fitting and B: corresponding DRT profiles.

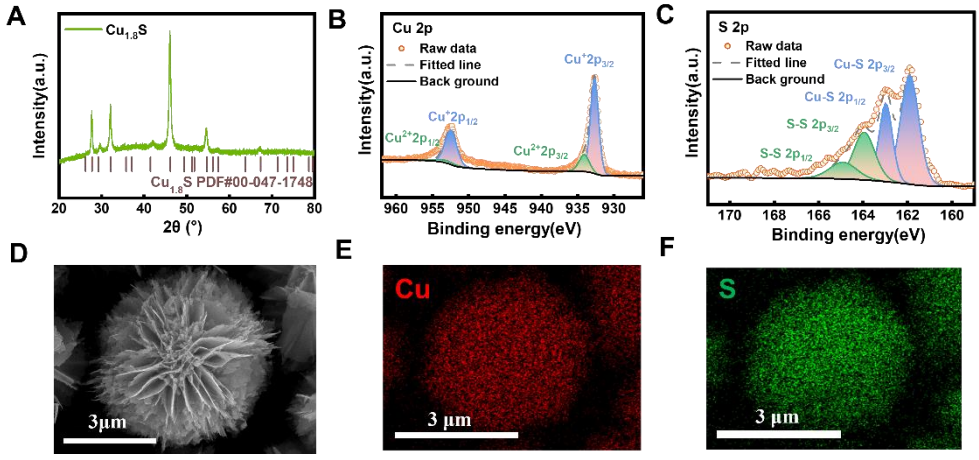

Supplementary Figure 12 A: XRD pattern of the $Cu_{1.8}S$ material; B: Cu 2p and C: S 2p XPS spectra; D: SEM image and E, F: the respective elemental mapping.

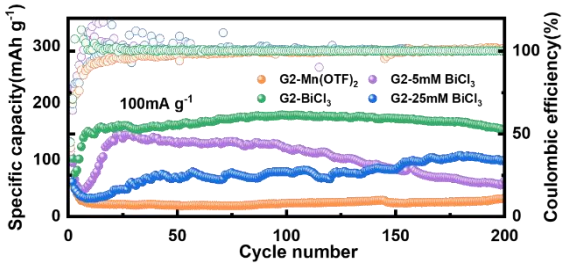

Supplementary Figure 13 Long-term cycling performance of Mn||$Cu_{1.8}S$ full cells with electrolytes containing different concentrations of $BiCl_3$ at a current density of 100 mA g^{-1}.

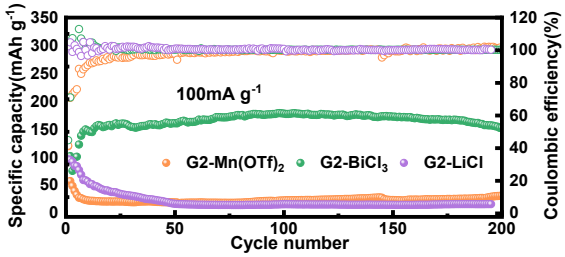

Supplementary Figure 14 Comparison of the specific capacities of Mn||$Cu_{1.8}S$ full cells employing G2-$Mn(OTf)_2$, G2-$BiCl_3$, and G2-LiCl electrolytes at 100 mA g^{-1}.

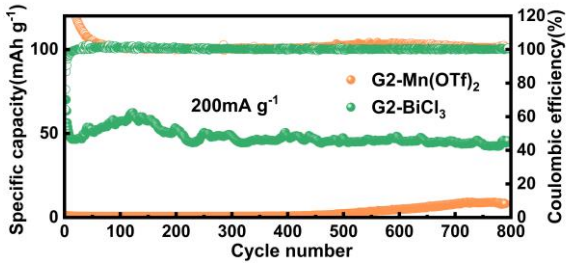

Supplementary Figure 15 Comparison of the cycling performance of Mn||$Cu_{1.8}S$ full cells employing G2-$Mn(OTf)_2$ and G2-$BiCl_3$ electrolytes at 200 mA g^{-1}.

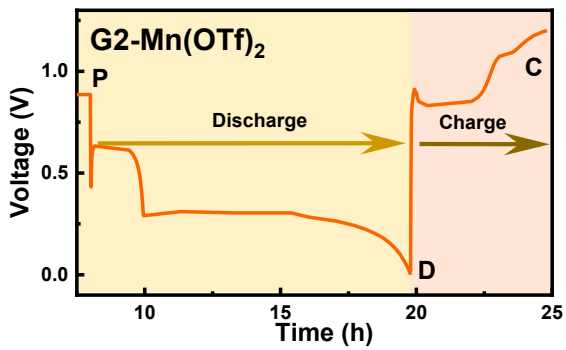

.

Supplementary Figure 16 Within the voltage range of 0 V to 1.2 V, GCD profile of the Mn||$Cu_{1.8}S$ full cell with G2-$Mn(OTf)_2$ electrolyte. The states selected for ex situ measurements are marked.

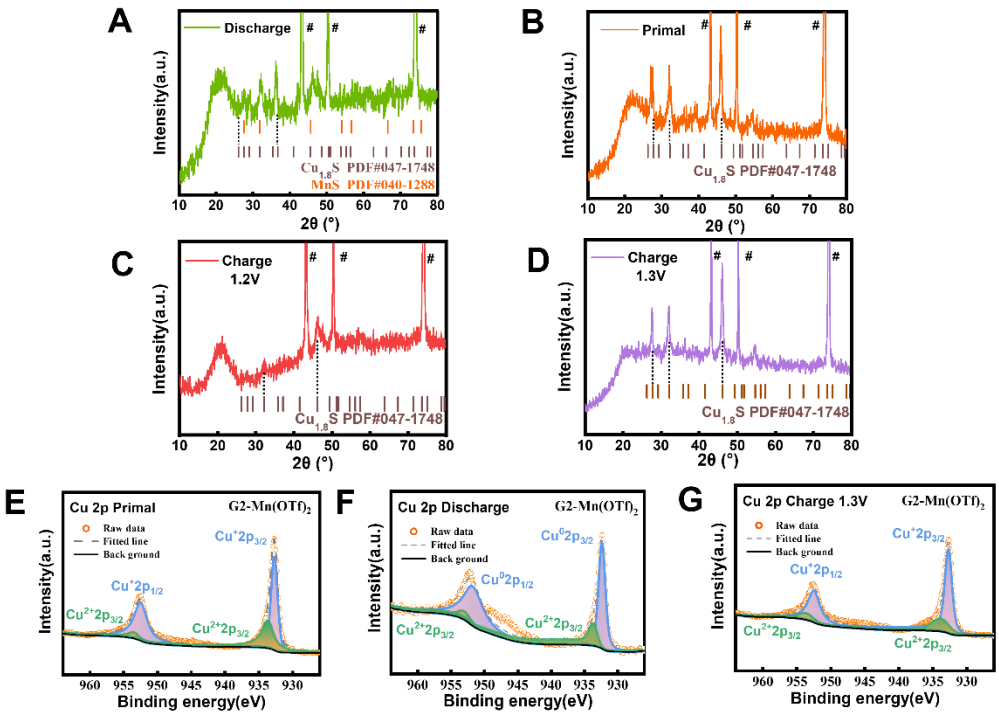

Supplementary Figure 17 A-D: Ex situ XRD patterns of the $Cu_{1.8}S$ cathode at different GCD states after cycling: A-C: Voltage range of 0-1.2 V; D: Voltage range of 0-1.3 V. The # marks in the figure correspond to the XRD of the Cu current collector; E-G: *Ex situ* XPS spectra of the Mn||$Cu_{1.8}S$ full cells at the corresponding states.